Generating Electric Field Test Patterns for Electric Grid Resiliency Studies

Melvin Stevens, Thomas J. Overbye, Jonathan Snodgrass, Adam B. Birchfield
Dept. of Electrical and Computer Engineering
Texas A&M University, College Station, TX, USA
mrsteven@tamu.edu, overbye@tamu.edu, snodgrass@tamu.edu, abirchfield@tamu.edu,

***Abstract*—** The world's electric grids are susceptible to geomagnetic phenomenon such as disturbances created by coronal mass ejections (CMEs) from the sun, which create geomagnetically induce currents (GICs) in the systems. It is important to study events such as geomagnetic disturbances (GMDs) to ensure the electric grids' resiliency against such events. In this work, test patterns of time varying electric fields are proposed to assist with the study of GMDs and other electromagnetic phenomena which may affect the stability of the power grids. Formulation of mitigation strategies against electromagnetic events which may cause major grid issues, such as system voltage collapse and transformer overheating is the focus of this work.

***Keywords*—** Geomagnetic disturbance (GMD), geomagnetically induced currents (GICs), test patterns

I. INTRODUCTION

Electrical grids are foundational to modern life; and are, arguably, the most critical systems operating today. In order to ensure a high standard of living, precedence should be given to investigating and fortifying the resiliency of the electrical grids upon which these services rely. This includes considering the impact of severe events that have the potential for large-scale, long-term outages, what are often called High-Impact, Low Frequency events (HILFs) [1]. The focus of this paper is one type of HILF, geomagnetic disturbances (GMDs).

GMDs, which are caused by corona mass ejections (CMEs) from the sun interacting with the earth's magnetic field, can impact large-scale electric grids by causing quasi-dc (i.e., frequencies much less than 1 Hz) electric fields on the earth's surface that can in turn cause geomagnetically induced currents (GICs) in high voltage transmission lines.

The potential for GMDs to impact large-scale electric grids has been known since at least the early 1940's [2], with [3] mentioning that in 1940 Philadelphia Electric Company recorded strong GMD-induced reactive power swings and voltage surges throughout their grid. In March 13-14, 1989 a large CME, which caused northern lights (aurora borealis) visible as far south as the US states of Texas and Florida, caused a blackout that affected almost the entire province of Quebec [4] with the GMD lasting for many hours with varying degrees of intensity. A much larger GMD, known as the Carrington event, occurred in 1859 [5] before the development of electric grids.

Over the last several decades, especially the last 15 years, there has been good progress in better understanding and modeling the impacts of GMDs on electric grids. However, an ongoing need, and the subject of this paper, is the development of additional electric field test patterns to help with the development of GMD mitigation strategies. The remainder of the paper is organized as follows. The next section provides some background on GMD analysis and mitigation. The following section then provides some results on the implementation and application of some new test patterns. The final section provides a conclusion and future directions.

II. BACKGROUND

As noted in [6], in doing GMD planning studies there are two primary issues that need to be considered. The first is to assess the risk of the grid to voltage limit violations, potential voltage collapse, and cascading outages considering the impact of the increase transformer reactive power consumption cause by half-cycle saturation due to the GICs. This is done by solving a GIC-enhanced power flow, with a first implementation given in [7], and then [8] providing further details and application to large grids.

A key input to this power flow is an assumed spatially-varying electric field. While the initial implementations assumed a uniform electric field, more recent applications, including those used in the North America for required GMD assessment studies [9], use a spatially-varying electric field magnitude [10]. Often the magnitude is varied by the product of a term that depends on the geomagnetic latitude (denoted as α) and a term that accounts for the variation in the ground conductivity (denoted as β). The electric field magnitude is also sometimes increased in smaller regions (a few hundred kilometers or less) in a process known as enhancement.

For each power flow solution, a uniform electric field direction is usually assumed. However, since it has long been known that the assumed electric field direction can substantially impact the results [11], different uniform directions are usually modeled. Since, for a uniform direction electric field the GICs are a linear function of the field, worst case directions can be analytically determined from just two power flow solutions.

The second GMD issue considered in a planning study is to assess the thermal impacts on equipment, particularly high voltage transformers, due to the GICs within the device. However, since the thermal impacts in transformers usually have time constants on the order of 5 to 20 minutes, their assessment requires assumptions about the time variation in the electric field. Thermal impact screening can be done in

three different ways [6]: 1) use transformer manufacturer GIC capability curves that require a peak GIC obtained from a power flow solution at the maximum electric field value, 2) generic GIC capability curves that assume a particular electric field time variation and a peak field power flow solution, or 3) use an assumed time-varying electric field to perform a series of power flow solutions and use the approach of [11] to determine the thermal impacts.

Both the voltage stability and thermal assessments require an assumed electric field test pattern. While there has been lots of work done in replicating previous storms (with examples including [5], [12], [13], and [14]), there are currently no test patterns available that replicate the full spatial and temporal electric field variation that could occur during a GMD. Hence the purpose of this paper.

One test pattern that is available and widely used is the one developed by North American Electric Reliability Corporation (NERC) for its new standard [9]. Known as the benchmark event, it is based upon the March 13-14, 1989 GMD event as measured at a geomagnetic observatory in Ontario [15]. The event consists of 31 hours of ten second data, with two values at each time point expressed in rectangular coordinates – the electric field in the eastward direction, E_y, and in the northward direction, E_x, with their values scaled so the peak value is 8 V/km. Alternatively the values could be expressed in polar coordinates as a magnitude and direction. Figure 1 shows a plot of the electric field magnitude over this entire period, with the electric field variability readily apparent; the maximum occurs at hour 25.3. Figure 2 then plots the electric field compass angle (i.e., north is 0°, east is 90°, etc.) over just the hour with the maximum value. The variability in the angle is also apparent, keeping in mind that the degrees wrap around so 0° and 360° are the same direction.

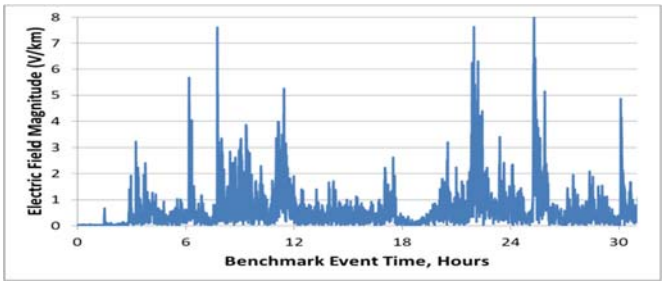

Figure 1: NERC Benchmark Electric Field Magnitude

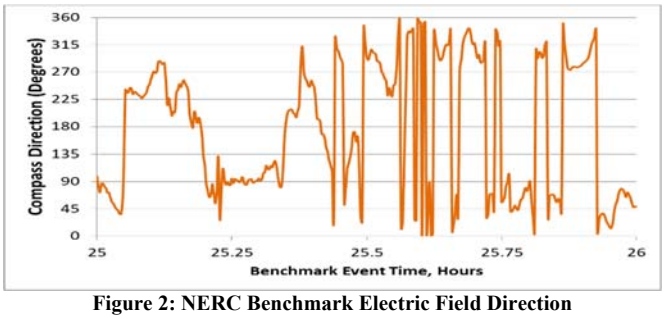

Figure 2: NERC Benchmark Electric Field Direction

Clearly this benchmark event is a well-considered and useful test pattern especially for the thermal assessments. However, there are three reasons associated with the need for additional test patterns. First, currently it is the only one. While it has the advantage of representing an actual GMD event, a future storm will certainly be different, and could be substantially different.

Second, it only has a single electric field complex value per time point. While the previously mentioned α and β values do vary the magnitude, at a particular geographic location they are constant. More variability is provided by the field enhancement; however, it is still usually done assuming a uniform electric field direction albeit with consideration of a number of different directions. While this approach can be quite helpful, it is easy to construct examples in which it underestimates the GICs for some transformers. As example, consider the six-bus grid shown in Figure 3, which slightly modifies the four-bus example from [16] by adding a new bus and transformer midway between Bus 1 and Bus 2. In the example all the buses have the same latitude, so a north-south field would be perpendicular to the transmission line and no GIC-voltage would be induced. For a uniformly directed field the worst-case direction is east-west, such as with the Figure 3 1 V/km field result which matches that from [16], with no GICs flowing in the Bus 5-6 transformer. However, if a non-uniform direction field is assumed, still at 1 V/km, the worst-case situation is shown in Fig 4, now with a higher value of GICs in the Bus 5-6 transformer than in either of the other transformers previously. While having electric fields flowing in different directions might seem extreme, it is a pretty good approximation to what can occur when the electric fields are created by a high-altitude electromagnetic pulse (HEMP) E3 event, with [17] showing an example HEMP E3 waveform and [18] a synthetic one. The amount of spatial variability that could occur during a large GMD may likely be unanticipated.

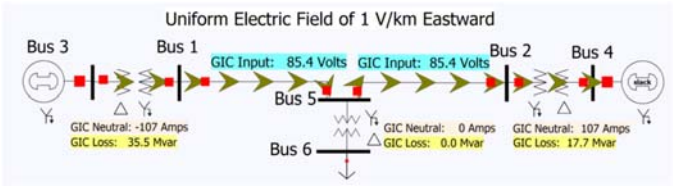

Figure 3: Six-Bus Example with a Uniform Direction Electric Field

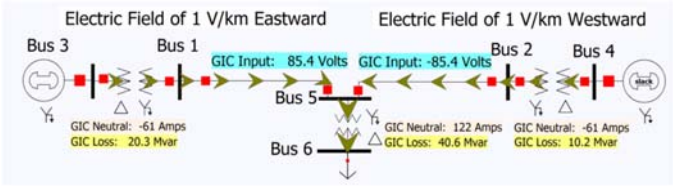

Figure 4: Six-Bus Example with a Non-Uniform Direction Electric Field

Third, existing uniform direction test patterns do not likely capture the amount of electric grid variability that could occur during an actual GMD. As shown in Figure 3 and Figure 4, as the electric field direction changes, the GICs and the associated system impacts could vary substantially. This variability is usually not fully captured with a uniform direction approach. Also, uniform direction fields tend to push the GICs to the system boundaries. This can be shown by

introducing a 2000 bus synthetic grid that covers most of Texas used in the remainder of the paper. Details on the creation of this grid are given in [19], while the full model is available at [20]. Figure 5 shows a oneline of this grid in which a 5 V/km uniform eastward electric field is modeled. The figure uses oval geographic data views (GDVs) [21] to show the substation sources and sinks for GICs with red ovals used to indicate locations where the GICs are moving from the ground into the grid and green ovals where the flow is into the ground; the oval size is proportional to the flow. The figure also visualizes the flow of the GICs using brown arrows. The west to east flow is clearly visible. An issue with this uniform direction approach is it could overestimate the GIC impacts at the boundaries and under estimate them in the rest. Another issue is associate with the development of GMD mitigation strategies. If an approach is developed just assuming a specific direction, or families of directions, it would likely not be optimal and may not even be beneficial if there is a large amount of variation. Hence the need for the creation of a variety of different electric grid test patterns.

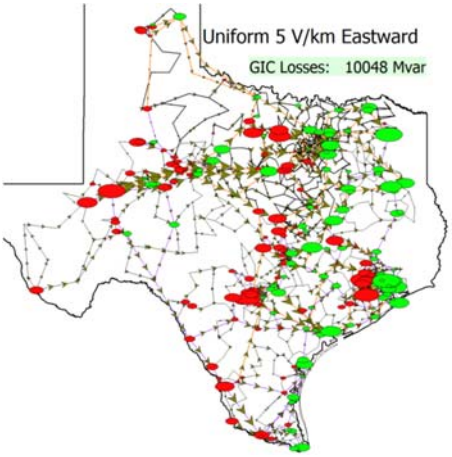

Figure 5: 2000-Bus Synthetic Grid GIC Visualization

III. IMPLEMENTATION AND RESULTS

Building on this background, this section introduces some GMD test patterns, and provides some preliminary analysis. There are, of course, many different approaches that could be taken in this test pattern development, and certainly a key consideration is the ultimate application. One approach, used by NERC, is to utilize an existing event to develop a benchmark event that can used to demonstrate compliance with a standard. An alternative approach, presented here, is to develop a variety of test patterns that can be used to help develop and assess the robustness of GMD mitigation strategies, including operator actions. With this approach the characteristics generally derived from prior GMDs, but are not meant to represent any previous event. Rather, the goal is they have sufficient variability to encompass what could occur in a wide variety of severe GMDs.

Key design considerations are the duration of the event, the ultimate electric field magnitude, and the frequency spectrum of the variation. For the duration, given that GMDs may last for days, any particular event could extend for many hours. However, with a focus on mitigation, and with the observation from prior events that the most severe electric fields tend to last much less than an hour, a shorter time period could be used. For the magnitude, certainly a large amount of guidance is provided by [10]. So, the maximum values could be similar to those of the NERC waveform, in which the goal is to have a "pass/fail" methodology. Alternatively, a scenario could be designed to "test to failure" in which the electric field is gradually increased until the grid is guaranteed to fail. The advantage of such an approach is it provides a helpful metric for the robustness of a mitigation strategy. The criteria is the frequency spectrum of variation. Here, Fast Fourier Transform (FFT) results from prior GMDs can be helpful with values generally below 5 mHz.

A general model for candidate test patterns is given below in equations (1) and (2), with the electric field specified in the previously mentioned rectangular coordinates, E_y and E_x.,

$$E_y(n,t,lat,lon) = \sum_{n=0}^{N} (A_{yn}\phi(lat,lon)\cdot F(\omega_{yn}t + \theta_{yn} + \nu_{yn}\lambda_y(lat,lon)) \quad (1)$$

$$E_x(n,t,lat,lon) = \sum_{n=0}^{N} (A_{xn}\phi(lat,lon)\cdot F(\omega_{xn}t + \theta_{xn} + \nu_{xn}\lambda_x(lat,lon)) \quad (2)$$

In equations (1) and (2) A is the base amplitude of the test pattern to be generated; for this work and the example test patterns describe later, A is chosen such that the generated test patterns are comparable to the NERC waveform in amplitude. The amplitude (spatial) scaling and phase (temporal) shifting functions $\phi(lat,lon)$ and $\theta + \nu\lambda(lat,lon)$ of equations (1) and (2) could be obtained from data associated with prior GMDs. Finally, F is a sinusoidal function, usually sine or cosine, ω_{xn} is the angular frequency of each sinusoid, and N is the number of sinusoids to be included in the test pattern.

Simulations of different test patterns are performed using the Texas 2k case, with various latitudinal and longitudinal grid configurations. Following, are the descriptions of two independent example test patterns, both simulated on a 0.5 x 0.5 latitudinal x longitudinal scaling grid. Using the model in (1), (2), and setting $N = 1$, the first example model in equations (3) and (4) are obtained; this first single frequency test pattern is generated and simulated using the Texas 2000 bus synthetic grid [20] . In the single frequency model described by equations (3) and (4), as well as the int multi-frequency model of equations (6) and (7), the amplitude scaling, and time shifting function are defined as affine functions of only latitude and longitude respectively, but not both, e.g. $\phi(lat)$ and $\theta + \nu\lambda(lon)$. In these models, $N = 1$ and $N = 3$ for the two respective test patterns. The base amplitude is set to $A = 7$ for the single frequency test pattern and $A = 4.5$ for the multiple frequency test pattern, to keep the test patterns similar in magnitude to NERC benchmark, a value of

8 V/km at a latitude of about 36º (i.e., the far north part of the footprint). The latitudinally and longitudinally dependent affine function for these initial electric field test patterns, $-1.733 + 0.073 \cdot lat$ and $(26.563 + 0.248) \cdot lon$, were obtained from the linear regression of points laid on a 0.5 lat x 0.5 lon grid of latitudinal and longitudinal coordinates that cover the state of Texas, US. In equation (4) $r1$ is a random number generator given in equation (5). The $random(0.92..1)$ function generates random numbers in the interval $[0.92, 1]$. The introduction of $r1$ allows the angle of the electric field to locationally vary. The 0.3 scaling factor in (5) is chosen to limit the phase difference between E_y and E_x.

$$E_y(t, lat, lon) = 7 \cdot (-1.733 + 0.073 \cdot lat) \cdot \cos(2\pi \cdot 0.001 \cdot t + 26.563 + 0.248 \cdot lon) \; V/km \quad (3)$$

$$E_x(t, lat, lon) = 7 \cdot (-1.733 + 0.073 \cdot lat) \cdot \cos(2\pi \cdot 0.001 \cdot t + r1 \cdot (26.563 + 0.248) \cdot lon) V/km \quad (4)$$

$$r1 = 0.3 \cdot 7 \cdot random(0.92..1) \quad (5)$$

Figure 6 shows both the temporal and spatial variations in the synthetic electric field imposed on the Texas 2k Synthetic case. The E-Field direction during the one-hour simulation time is shown in Figure 7; Figure 8 is a contour of the electric field, displaying its magnitude and direction. The bus voltages of the simulation are represented in Figure 9, with a snapshot of a contour of the same in Figure 10. Finally, the GICs flowing in the transformers' neutrals is plotted in Figure 11. Attention may be drawn to excessive voltage on a couple of buses at the end of the simulation in Figure 9 and Figure 15. This may be due to switched shunts at those buses; but further investigation would confirm this.

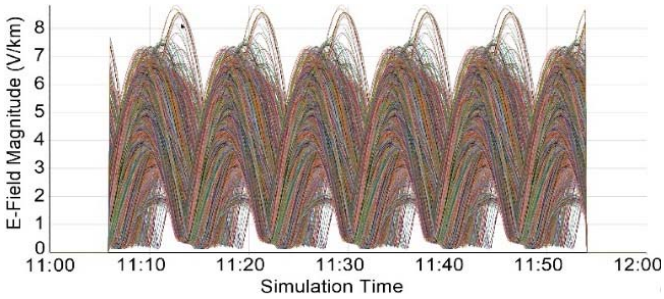

Figure 6: Test Pattern of a Single-Frequency Sinusoidal Electric Field Described by Equations (3) & (4) Applied to Texas 2K bus Synthetic Grid

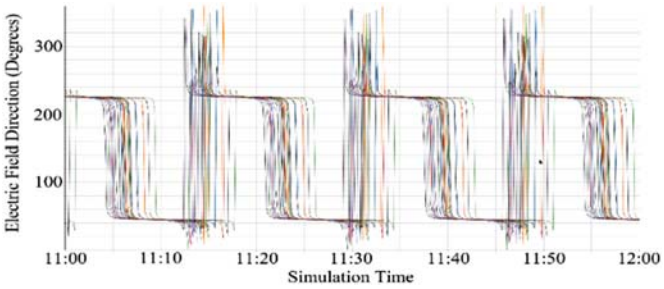

Figure 7: E-Field Direction of the Test Pattern of Figure 6

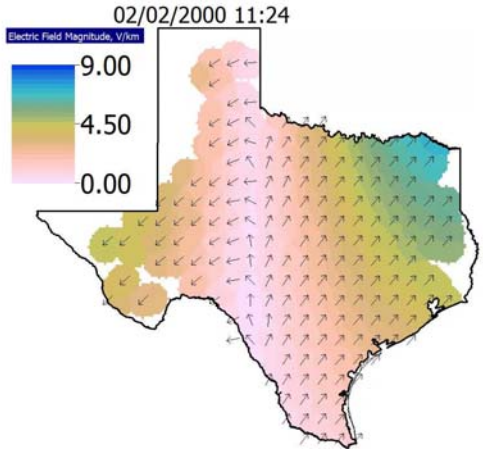

Figure 8: Contour and Direction of the Electric Field Test Pattern Generated by Equations (3) and (4) imposed on Texas 2k Synthetic Grid,

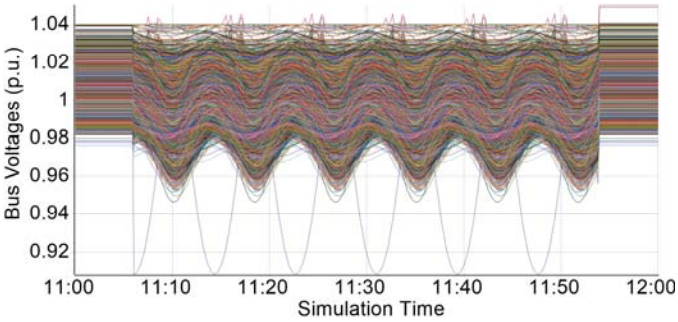

Figure 9: Bus Voltages in the Texas 2k Synthetic grid After Simulation, imposing the E-Field Test Patten in Figure 6

Equations (6) and (7) are used to generate the second test pattern plotted in Figure 12, which illustrates the E-field at the buses in the Texas 2k Synthetic Grid and Figure 13 plots the direction of the same. Figure 14 shows a contour of the multi-frequency E-Field test pattern. Figure 15 and Figure 16 illustrates the bus voltages and a snapshot of the voltage contour of the system respectively.

$$E_y(t, lat, lon) = 9 \cdot (-1.733 + 0.073 \cdot lat) \cdot \cos(2\pi \cdot 0.001 \cdot t + 26.563 + 0.248 \cdot lon) + 3 \cdot (-1.733 + 0.073 \cdot lat) \cdot \cos(10\pi \cdot 0.001 \cdot t + 26.563 + 0.248 \cdot lon) + 0.9 \cdot (-1.733 + 0.073 \cdot lat) \cdot \cos(18\pi \cdot 0.001 \cdot t + 26.563 + 0.248 \cdot lon) \quad (6)$$

$$E_x(t, lat, lon) = 9 \cdot (-1.733 + 0.073 \cdot lat) \cdot \cos(2\pi \cdot 0.001 \cdot t + r1 \cdot (26.563 + 0.248) \cdot lon) + 3 \cdot (-1.733 + 0.073 \cdot lat) \cdot \cos(10\pi \cdot 0.001 \cdot t + r1 \cdot (26.563 + 0.248) \cdot lon) + 0.9 \cdot (-1.733 + 0.073 \cdot lat) \cdot \cos(32\pi \cdot 0.001 \cdot t + r1 \cdot (26.563 + 0.248) \cdot lon) \quad (7)$$

Finally, Figure 17 shows the GICs flowing in the neutral

conductors of the transformers in the Texas 2k Synthetic Grid caused by the test pattern generated by (6) and (7). This second test pattern includes the fundamental frequency, and a few other frequencies to add some additional variation to the generated electric field.

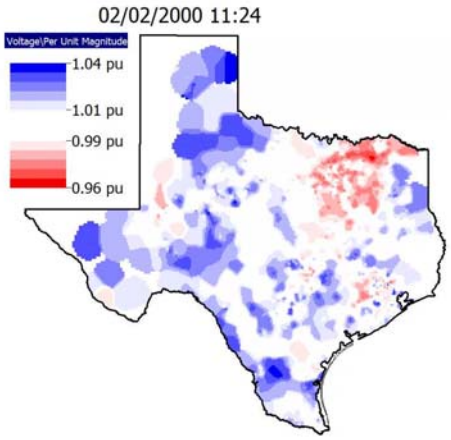

Figure 10:Snapshot of the Voltage Contour of Texas 2k Synthetic Grid due to the applied Electric Field Test Pattern of Figure 6

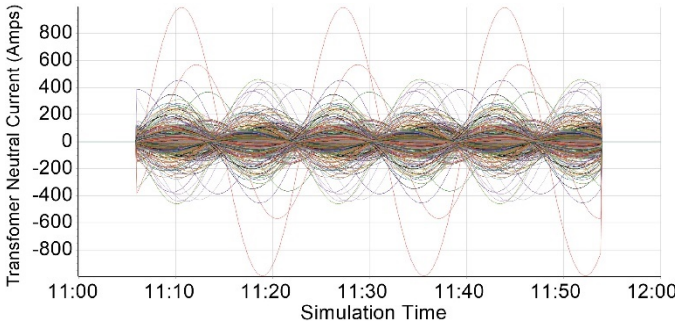

Figure 11: Transformer Neutral GICs Resulting from the Simulation of the Single Frequency Electric Field Test Pattern in Figure 6

The scaling factors in the second model, (6), (7), are chosen to ensure the test pattern generated would be similar to the NERC benchmark and the additional fifth and ninth harmonics chosen in equation (6) and the additional fifth and sixteenth harmonics found in equation (7) are chosen to add some variation to the test pattern in E_y and E_x from the fundamental frequency.

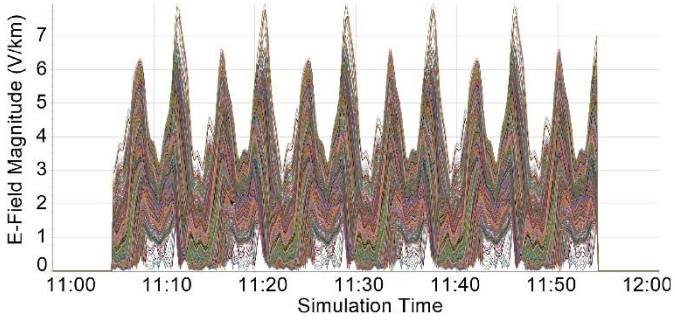

Figure 12: Multiple Frequency Electric Field Test Pattern Generated by Equations (6) and (7) Applied to Texas 2K bus Synthetic Grid.

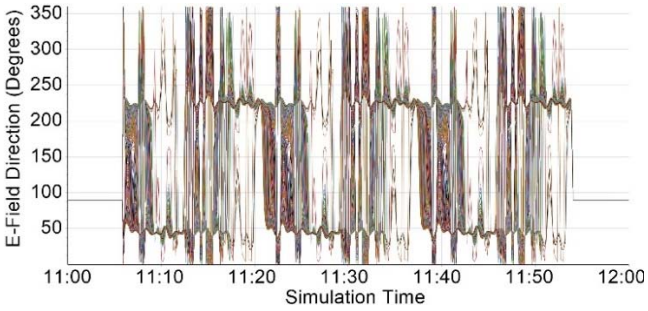

Figure 13: E-Field Direction of the Test Pattern of Figure 12

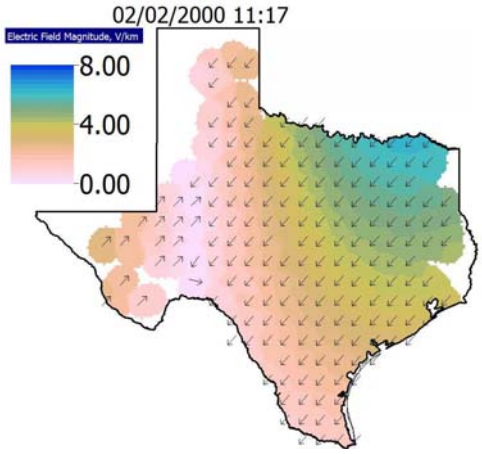

Figure 14: Contour and Direction Electric Field Test Pattern Generated by Equations (6) and (7) imposed on Texas 2k Synthetic Grid

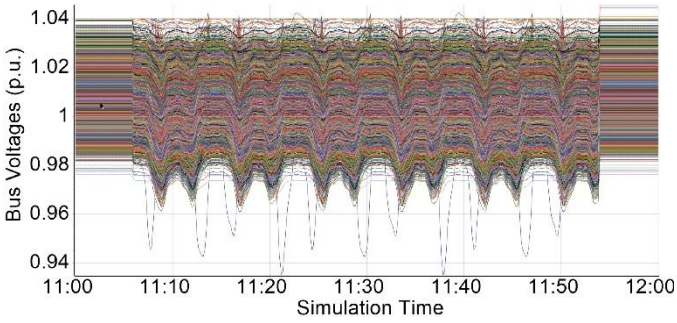

Figure 15: Bus Voltages in the Texas 2k Synthetic Grid Caused by the E-Field Test Patten in Figure 12

IV. CONCLUSIONS AND FUTURE WORK

For this initial work, the results given approximate a GMD event as sinusoidal waveforms. The first example test pattern is composed solely of a single frequency and the second test pattern discussed includes a total of three frequencies. Synthetic electric grids were then subjected to the test patterns and results were shown. Future work will include the analysis of more GMD events to assist in the production of more complex test patterns, which will be more similar to analyzed GMD. Those similarities will be in the principal components of past GMD events, i.e., the prominent frequencies and phases of the constituent sinusoids, of real GMD events. Some GMD test patterns will be designed to stress test power grids to the point of failure, conceivably voltage collapse.

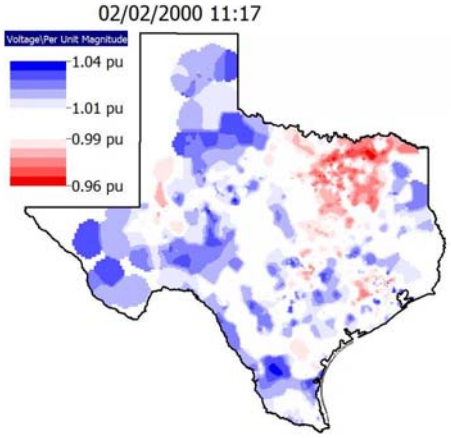

Figure 16: Snapshot of the Voltage Contour of the Texas 2k Synthetic Grid due to the applied Electric Field Test Pattern of Figure 12

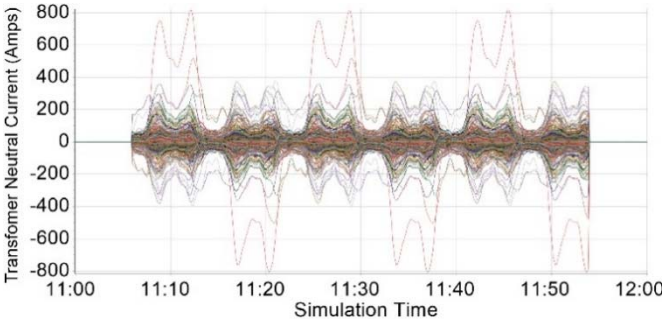

Figure 17: GICs Induced in the Neutrals of the Transformers in the Texas 2k Case by the E-Field Test Pattern generated by (6) and (7)

Having electric field test patterns that varied both in time and in space is a goal of this work; therefore, generated test patterns are phase shifted and magnitude scaled. The scaling and shifting functions for the geoelectric field are chosen to be affine functions; because, it was determined that the NERC recommended ground conductivity model had little to no effect on varying the geoelectric field in time and in space in certain geographical regions, particularly those of lower latitudes. For future work a ground conductivity model may be employed, there will be an increase in the number of frequencies used in the test patterns, E-field directions will be more varied

This research focuses not only on generating electric field test patterns, but also provides simulations of those synthetic electric field test patterns to support the main goal of the formulation and testing of mitigation strategies of GMD events that may have huge adverse effects on the worlds power grids. Since geomagnetic and geoelectric disturbances affect electric grids on a wide area basis it is vital to be proactive in devising mitigation strategies against them. This paper described this work toward the effort to derive mitigation strategies against future GMD events.

V. ACKNOWLEDGMENTS

This work was partially supported through funding provided by the US Department of Energy.

REFERENCES

[1] *High-Impact, Low Frequency Event Risk to the North American Bulk Power System*, North American Electric Reliability Corporation (NERC) and U.S. Department of Energy (DOE), June 2010.

[2] V. D. Albertson, J. M. Thorson, Jr., R.E. Clayton, S.C. Tripathy, "Solar-induced-currents in power systems: Cause and effects," *IEEE Trans. Power App. Syst.*, vol. PAS-92, no. 2, pp. 471–477, Mar./Apr. 1973.

[3] *Geomagnetic Disturbance Monitoring Approach and Implementation Strategies*, U.S. Department of Energy (DOE), January 2019.

[4] J. G. Kappenman, V.D. Albertson, "Bracing for the Geomagnetic Storms," *IEEE Spectrum*, vol. 27, pp. 27-33, March 1990.

[5] E. W. Cliver, W. F. Dietrich, "The 1859 Space Weather Event Revisited: Limits of Extreme Activity," *Journal of Space Weather and Space Climate*, vol. 3, p. A31, 2013.

[6] *Geomagnetic Disturbance Planning Guide*, North American Electric Reliability Corporation (NERC), Dec. 2013.

[7] V.D. Albertson, J.G. Kappenman, N. Mohan, G.A. Skarbakka, "Load-flow studies in the presence of geomagnetically induced currents," IEEE Trans. Power App. Syst., vol. PAS-100, pp. 594–606, Feb. 1981

[8] T. J. Overbye, T. R. Hutchins, K. Shetye, J. Weber, S. Dahman, "Integration of geomagnetic disturbance modeling into the power flow: A methodology for large-scale system studies," Proc. 2012 North American Power Symp., Champaign, IL, USA, Sep. 2012.

[9] "Transmission System Planned Performance for Geomagnetic Disturbance Events," NERC TPL-007-4, North American Electric Reliability Corporation, 2020.

[10] *Benchmark Geomagnetic Disturbance Event Description*, North American Electric Reliability Corporation, May 2016.

[11] L. Marti, A. Rezaei-Zare, A. Narang, "Simulation of Transformer Hotspot Heating due to Geomagnetically Induced Currents," *IEEE Transactions on Power Delivery*, , vol.28, no.1, pp.320-327, Jan. 2013.

[12] M.D. Butala, M. Kazerooni, J.J. Makela, F. Kamalabadi, J.L. Gannon, H. Zhu, T.J. Overbye, "Modeling Geomagnetically Induced Currents from Magnetometer Measurements: Spatial Scale Assessed with Reference Measurements," *Space Weather*, Vol. 15, 1357–1372, 2017.

[13] S. Vennerstrom, et. al., "Extreme geomagnetic storms–1868–2010," *Solar Physics*, vol. 291, pp. 1447–1481, 2016.

[14] L.H. Wei, N. Homeier, J.L. Gannon, "Surface Electric fields for North America During Historical Geomagnetic Storms," *Space Weather*, vol. 11, pp. 451-462, July 2013.

[15] *Benchmark Geomagnetic Disturbance Event Description*, North American Electric Reliability Corporation, May 2016.

[16] K. Shetye and T.J. Overbye, "Modeling and Analysis of GMD Effects on Power Systems: An overview of the impact on large-scale power systems," IEEE Electrification Mag., vol. 3, Issue 4, 2015, pp. 13-21.

[17] Nominal Waveforms for Late-Time High-Altitude Electromagnetic Pulse (HEMP), DTRA-TR-19-41, Applied Research Associates, September 2019; available at apps.dtic.mil/sti/pdfs/AD1082958.pdf.

[18] T.J. Overbye, J. Snodgrass, A.B. Birchfield, M. Stevens, "Towards Developing Implementable High Altitude Electromagnetic Pulse E3 Mitigation Strategies for Large-Scale Electric Grids," Texas Power and Energy Conference (TPEC), College Station, TX, March 2022.

[19] A.B. Birchfield, T. Xu, K. Gegner, K.S. Shetye, T.J. Overbye, "Grid Structural Characteristics as Validation Criteria for Synthetic Networks," *IEEE Trans. Power Syst.*, vol. 32, pp. 3258-3265, July 2017.

[20] Texas A&M University Electric Grid Test Case Repository, electricgrids.engr.tamu.edu

[21] T.J. Overbye, J.L. Wert, K.S. Shetye, F. Safdarian, and A.B. Birchfield, "The Use of Geographic Data Views to Help With Wide-Area Electric Grid Situational Awareness," IEEE Texas Power and Energy Conference, College Station, TX, Feb. 2021.